Roark, D. E., & Yphantis, D. A. (1969) *Ann. N.Y. Acad. Sci. 164*, 245.
Sanwal, B. D., & Stachow, C. S. (1965) *Biochim. Biophys. Acta 96*, 28.
Sanwal, B. D., & Cook, R. A. (1966) *Biochemistry 5*, 886.
Sanwal, B. D., Zink, M. W., & Stachow, C. S. (1963) *Biochem. Biophys. Res. Commun. 12*, 510.
Sanwal, B. D., Zink, M. W., & Stachow, C. S. (1964) *J. Biol. Chem. 239*, 1597.
Sanwal, B. D., Stachow, C. S., & Cook, R. A. (1965) *Biochemistry 4*, 410.
Siepen, D., Yu, P.-H., & Kula, M.-R. (1975) *Eur. J. Biochem. 56*, 271.
Taber, H. W., & Sherman, F. (1964) *Ann. N.Y. Acad. Sci. 121*, 600.
Thorun, W., & Maurer, H. R. (1971) in *Disc Electrophoresis and Related Techniques of Polyacrylamide Gel Electrophoresis* (Maurer, H. R., Ed.) pp 8–17, Walter de Gruyter, Berlin.
Vogel, H. J. (1956) *Microb. Genet. Bull. 13*, 42.
Weber, K., & Osborn, M. (1969) *J. Biol. Chem. 244*, 4406.
Weber, K., Pringle, J. R., & Osborn, M. (1972) *Methods Enzymol. 26*, 3.
Yphantis, D. A. (1964) *Biochemistry 3*, 297.
Yu, P.-H., Kula, M.-R., & Tsai, H. (1973) *Eur. J. Biochem. 32*, 129.

Kinetics of Association between Bisquaternary Ammonium Ligands and Acetylcholinesterase. Evidence for Two Conformational States of the Enzyme from Stopped-Flow Measurements of Fluorescence†

Michael B. Bolger* and Palmer Taylor

ABSTRACT: Bisquaternary ammonium ligands in which the quaternary groups are separated by 14 Å are known to bind with high affinity to acetylcholinesterase. A series of bisquaternary ligands containing a benzoquinone moiety exhibit absorption spectra which overlap the fluorescence emission of the tryptophanyl residues on the protein. Upon complexation with acetylcholinesterase, quenching of protein fluorescence occurs along with a shift of emission maximum to shorter wavelength. The latter phenomenon suggests that a conformational change is associated with ligand binding. A study of the kinetics of complexation using stopped-flow instrumentation reveals that a rapid bimolecular step ($k = 9.7 \times 10^7$ M^{-1} s^{-1}) is followed by a relatively slow unimolecular ($k = 44$ s^{-1}) interconversion of enzyme species. The unimolecular step, which appears to involve an isomerization of two enzyme forms that exist prior to ligand binding, was found to occur for all the bisquaternary ligands examined. The kinetics of complexation, where a bimolecular rate below diffusion-controlled rates and a slow isomerization of the enzyme are observed, appear to be unique to the bisquaternary compounds since ligands which bind exclusively to the active center or peripheral anionic site exhibit association kinetics approximating that of a diffusion-controlled reaction. The change in conformation may well be associated with the necessity of obtaining the proper spatial arrangement between the two anionic sites on acetylcholinesterase at which the quaternary groups bind.

In recent years, it has become possible to measure the association of inhibitory ligands with acetylcholinesterase (AcChE)[1] by direct fluorescence (Mooser et al., 1972; Mooser & Sigman, 1974; Taylor & Jacobs, 1974; Taylor & Lappi, 1975) and magnetic resonance (Kato, 1972; Wee et al., 1976) techniques. These approaches have enabled investigators to confirm the existence of a peripheral site(s) for ligand binding which had previously been adduced from steady-state kinetic measurements of inhibition of substrate catalysis (Changeux, 1966). Hence, certain ligands such as edrophonium or the fluorescent compound *N*-methylacridinium will inhibit substrate hydrolysis by binding to the active center (Mooser et al., 1972) while other inhibitory compounds such as propidium at low ionic strength bind exclusively to a site peripheral to the active center (Taylor & Lappi, 1975). The stoichiometry of each ligand is 1:1 with the 80 000-dalton subunit on the tetrameric enzyme, and ternary complexes can be demonstrated where the respective ligands bind to the active and peripheral sites on each subunit (Mooser & Sigman, 1974; Taylor & Lappi, 1975). Bisquaternary ligands in which a 10 carbon methylene chain or approximately 14 Å separates the quaternary nitrogens are of particular interest since their binding is mutually exclusive with ligands that bind either to the peripheral site or to the active center (Taylor & Lappi, 1975). A complex where the bisquaternary ligand spans

† From the Division of Pharmacology, Department of Medicine, University of California, San Diego, La Jolla, California 92093. *Received February 2, 1979.* Supported in part by U.S. Public Health Service Grant 18360.
* M.B.B. was supported by U.S. Public Health Service Training Grant 02267 and National Institutes of Health Postdoctoral Fellowship GM-06410.

[1] Abbreviations used: AcChE, acetylcholinesterase; *o*ClB-BQ, 2,5-bis[[3-[diethyl(*o*-chlorobenzyl)ammonio]propyl]amino]benzoquinone; $p$$NO_2$B-BQ, 2,5-bis[[3-[diethyl(*p*-nitrobenzyl)ammonio]propyl]-amino]benzoquinone; B-BQ, 2,5-bis[[3-(diethylbenzylammonio)-propyl]amino]benzoquinone; DAP, 1,10-bis(3-aminopyridinio)decane; Et_3-BQ, 2,5-bis[[3-(triethylammonio)propyl]amino]benzoquinone; Me_3-BQ, 2,5-bis[[3-(trimethylammonio)propyl]amino]benzoquinone; *o*Br-ambenonium, *N*,*N*′-bis[[2-[diethyl(*o*-bromobenzyl)ammonio]ethyl]amino]-oxamide; ambenonium, *N*,*N*′-bis[[2-[diethyl(*o*-chlorobenzyl)ammonio]ethyl]amino]oxamide.

0006-2960/79/0418-3622$01.00/0

between the two sites can be considered as a possible mode of binding for these compounds. Several approaches could be utilized to investigate this possibility. Through fluorescence energy transfer with active center (Berman & Taylor, 1978) and peripheral site specific ligands, intersite distances could be measured to ascertain whether such distances are compatible with a flexible 14-Å ligand spanning between them. Since intersite distances would be measured in the absence of bisquaternary ligands, an investigation of the mechanism of ligand binding and the nature of possible conformational changes attendant to ligand binding become essential issues in describing the topography of bisquaternary ligand association with AcChE. A kinetic study of bisquaternary binding would prove enlightening in that it provides an operational test of the binding mechanism. Rosenberry & Neumann (1977) have found that *N*-methylacridinium, which associates predominately with the active center, binds at rates expected for a diffusion-controlled reaction. Their finding provides a valuable frame of reference for examining complex formation for the bisquaternary compounds whose mode of association appears more complex.

Certain bisquaternary ligands such as those of the benzoquinone series contain chromophoric groups suitable for quenching the protein tryptophanyl fluorescence by a dipolar transfer mechanism upon ligand complexation (Förster, 1965). In this study we have employed fluorescence monitoring and stopped-flow instrumentation to examine the kinetics of association and dissociation of these ligands with AcChE. Three separate lines of evidence are developed from the kinetic analysis to suggest that the enzyme exists in two conformational states prior to ligand binding.

Experimental Section

Materials. The 11S or lytic form of acetylcholinesterase (EC 3.1.1.7) was prepared as previously described (Taylor et al., 1974). The enzyme was stored in a high ionic strength buffer (0.1 M NaCl, 40 mM $MgCl_2$, and 10 mM Tris-HCl, pH 8.0) at −20 °C in polypropylene tubes for periods up to 4 months without loss of activity.

All of the bisquaternary benzoquinone derivatives and *o*-bromoambenonium were kindly supplied by Dr. F. C. Nachod of the Sterling-Winthrop Research Institute, Rensselaer, NY, and used without further purification. 1,10-Bis(3-aminopyridinio)decane was prepared and recrystallized from ethanol as described by Mooser et al. (1972) (mp 179–180.5 °C; lit. mp 180–181.5 °C). Propidium diiodide was obtained from Calbiochem and used without further purification.

Equilibrium Fluorescence Titrations. Equilibrium dissociation constants for complex formation were determined from titration of the AcChE tryptophanyl fluorescence ($\lambda_{excitation}$ = 290 nm; $\lambda_{emission}$ = 335 nm) as previously described (Taylor & Jacobs, 1974). The recorded values represent the means of at least three separate titrations. AcChE concentration is specified on the basis of subunit molarity by assuming a subunit molecular weight of 80 000.

Stopped-Flow Kinetic Methods. Association kinetics at 4 °C and all dissociation kinetics were measured with a Durrum Model D-110 stopped-flow spectrophotometer equipped with a Hamamatsu R-376 photomultiplier tube for fluorescence detection. A Corning CS 7-54 window filter (250–390 nm) was placed in the excitation beam while emitted light passed through a CS 0-54 cutoff filter. The cylindrical flow cuvette (0.2 × 2 cm) was modified by applying a thin silver coating to the lower half of the cuvette in order to maximize collection of the fluorescence signal. Temperatures around the cuvette

Chart I

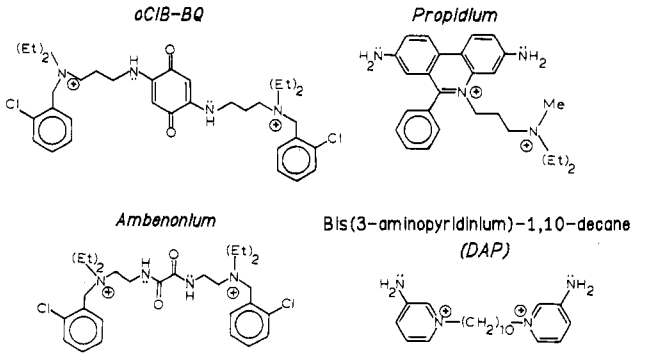

and drive syringes were maintained within ±1 °C by a circulating bath. Photographed traces from the storage oscilloscope were projected onto a Talos digitizing tablet so that digital data could be input directly to a Tektronix 4051 computer. The dead time of the instrument was found to be 2.5 ms by monitoring the enhancement of 8-anilino-1-naphthalenesulfonic acid fluorescence upon binding to bovine serum albumin. Mixing efficiency was tested by umbelliferone quenching and found to be complete within the instrumental dead time.

Observed rate constants greater than 400 s^{-1} were measured on an Aminco-Morrow stopped-flow instrument with a fast mixing cell designed by Dr. P. B. Chock. The instrument has been found to have a dead time of 500 μs (Rhee & Chock, 1976). Output signals were amplified, offset, filtered, and recorded on a Tektronix WP 1200 digital processing oscilloscope for signal averaging and plotting.

Curve-fitting calculations were performed on the digitized data with the Tektronix 4051 computer by the use of a general nonlinear least-squares regression analysis program based on Marquardt's method (Marquardt, 1963).

Results

Fluorescence Emission Spectra of the Complexes. As shown previously, 2,5-bis[[3-[diethyl(*o*-chlorobenzyl)ammonio]propyl]amino]benzoquinone (*o*ClB-BQ) (cf. Chart I) binds with a 1:1 stoichiometry with each 80 000-dalton subunit in the AcChE tetramer (Taylor & Jacobs, 1974). Fluorescence emission spectra of AcChE excited at 290 nm before and after addition of a saturating quantity of *o*ClB-BQ or *o*-bromoambenonium are shown in Figure 1. Tryptophanyl fluorescence (λ_{em} = 335 nm) is quenched ~50% by the benzoquinone derivative which shows maximal absorbance at 340 nm (ϵ_{340}^{M} = 2.5 × 10^4 M^{-1} cm^{-1}). Fluorescence emission of the complex is blue-shifted by 6 nm from 335 to 329 nm. *o*-Bromoambenonium, despite having no absorbance in the region of AcChE emission, causes slight (~19%) quenching of the tryptophanyl fluorescence with a smaller (3-nm) hypsochromic shift. The UV spectrum of *o*-bromoambenonium showed no contaminants which absorb at wavelengths near 340 nm (ϵ_{277}^{M} < 5 × 10^2). Thus, the reduction in quantum yield of the protein tryptophanyl residues and the shift in the emission maximum for the ambenonium–AcChE complex cannot be due to dipolar energy transfer which requires the spectral overlap between donor and acceptor ligands (Förster, 1965; Stryer, 1968). Hence, the spectral shift, which was also observed for ambenonium complexation, likely reflects a conformational change which alters the environment of some of the tryptophanyl residues in the AcChE–ligand complex.

Kinetics of Association between the Bisquaternary Ligands and AcChE. Typical oscilloscope recordings of the change in the fluorescence of 0.2 μM AcChE upon addition of either

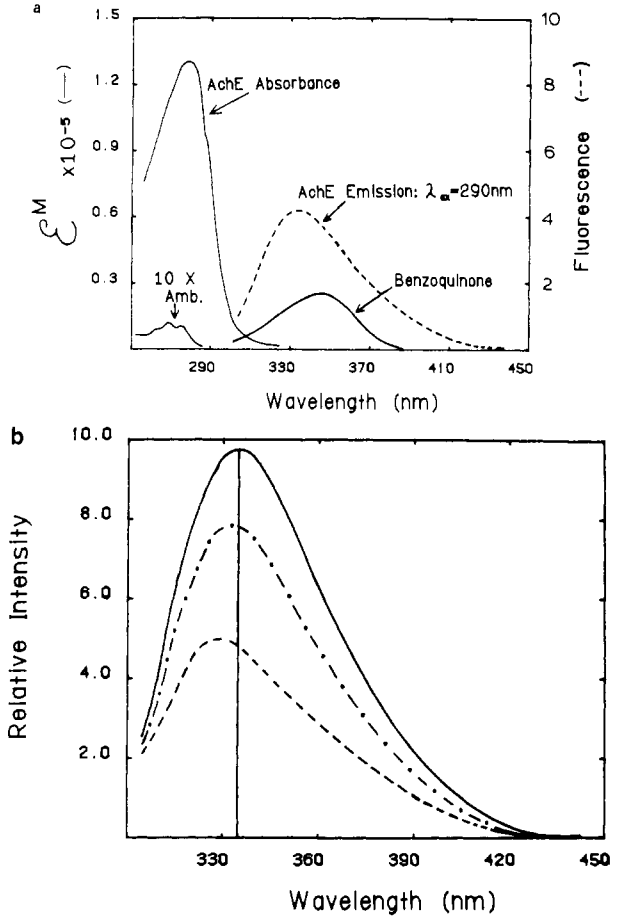

FIGURE 1: (a) Absorption and fluorescence emission spectra of acetylcholinesterase and absorption spectrum of 2,5-bis[[3-[diethyl(*o*-chlorobenzyl)ammonio]propyl]amino]benzoquinone and ambenonium. Spectra were recorded at 25 °C in a Cary 15 spectrophotometer and a Farrand spectrofluorometer with a corrected excitation accessory. Sample buffer was 0.1 N NaCl, 0.04 M $MgCl_2$, and 0.1 M Tris-HCl, pH 8.0. (b) Fluorescence emission spectra of acetylcholinesterase in the absence and in association with bisquaternary ligands. Spectra were recorded as described above with excitation at 290 nm. (—) Acetylcholinesterase alone (1 μM); (---) acetylcholinesterase (1 μM) and ambenonium (7.5 μM); (- - -) acetylcholinesterase (1 μM) and *o*ClB-BQ[1] (7.8 μM).

1 or 10 μM *o*ClB-BQ are shown in Figure 2a. Since the K_d for this ligand is around 28 nM (Taylor & Jacobs, 1974), it can be calculated that at the ligand concentrations represented, 97 and 99% of the AcChE sites would be bound with ligand, respectively. Instead of observing the anticipated pseudo-first-order kinetics, we found that two components to the fluorescence signal become manifest upon binding to the bisquaternary ligand. The rate of the faster component increases with ligand concentration while the slow component of fluorescence change is independent of ligand concentration. Nonlinear regression analyses were used to fit the digitized data to a double-exponential model (eq 1). The best fit curves

$$Y = A_1 e^{-k_1 t} + A_2 e^{-k_2 t} \quad (1)$$

in Figure 2b were generated by allowing the computer to optimize the parameters A_1, k_1, A_2, and k_2 so as to minimize the sum of the squared deviations between the model equation and the data until the change in either the parameter values or the sum of the squares was less than 10^{-4} and 10^{-5}, respectively. The final parameters k_1 and k_2 represent the fast and slow observed rate constants of the *o*-ClB-BQ binding reaction at 4, 9, and 25 °C and are plotted as a function of ligand concentration in Figure 3. An increase in the slope

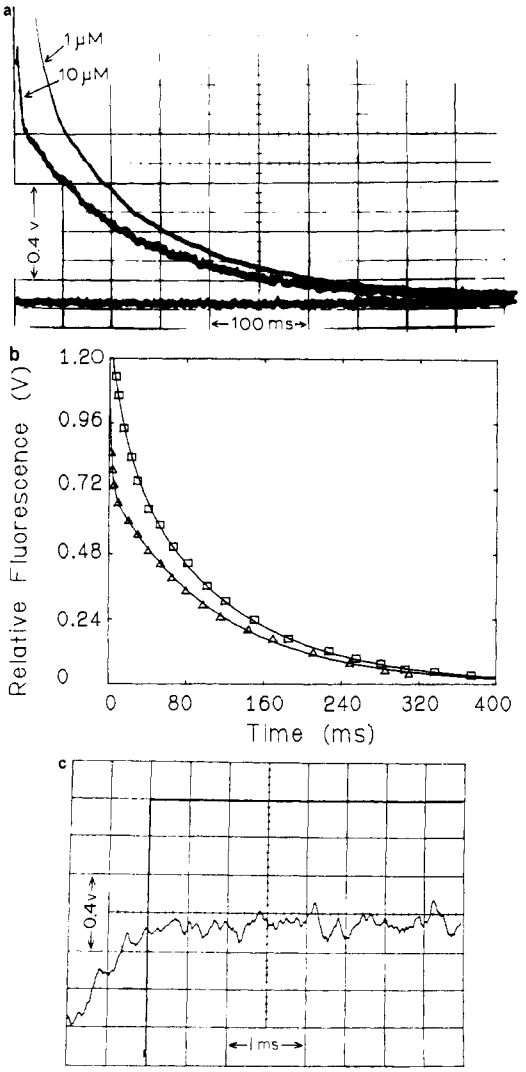

FIGURE 2: (a) Oscilloscope recording of the reaction of 0.2 μM AcChE with 1 and 10 μM *o*ClB-BQ at 4 °C. (b) Plot of the digitized data from Figure 2a with curves fit to a double-exponential model. (□) AcChE (0.2 μM) and *o*ClB-BQ (1 μM) double-exponential model parameters: $A_1 = 0.38$; $k_1 = 50\ s^{-1}$; $A_2 = 0.90$; $k_2 = 9\ s^{-1}$. (△) AcChE (0.2 μM) and *o*ClB-BQ (10 μM) double-exponential parameters: $A_1 = 0.36$; $k_1 = 430\ s^{-1}$; $A_2 = 0.72$; $k_2 = 9\ s^{-1}$. (c) Association between 1.0 μM propidium and 0.3 μM AcChE in 0.001 M Tris-HCl, pH 8.0, at 19 °C. Propidium fluorescence enhancement was measured with excitation at 535 nm.

Table I: Kinetic Constants and Respective Amplitudes Obtained for the Biphasic Reaction between 2,5-Bis[[3-[diethyl(*o*-chlorobenzyl)ammonio]propyl]amino]benzoquinone and Acetylcholinesterase

temp (°C)	fast component slope[a] ($M^{-1}\ s^{-1}$)	slow component intercept[b] (s^{-1})	% fast component[c]	% slow component
25	$9.7\ (\pm0.4) \times 10^7$	44 (±6)	62 (±18)	38 (±6)
9	$6.2\ (\pm0.5) \times 10^7$	11 (±2)	39 (±9)	61 (±6)
4	$3.9\ (\pm0.7) \times 10^7$	9 (±0.4)	32 (±6)	68 (±7)

[a] Slopes were determined from Figure 3. Confidence interval = $(\pm t_{0.01(2),DF}) \times$ (standard error of slope). [b] Mean intercept and standard deviation assuming a slope of zero. [c] Relative amplitudes were determined for six concentrations (1–10 μM) from the amplitude parameters for the double-exponential model (Figure 2b).

of the fast component and in the intercept for the slower component is observed as the temperature increases. The slower component of the fluorescence quenching exhibits a

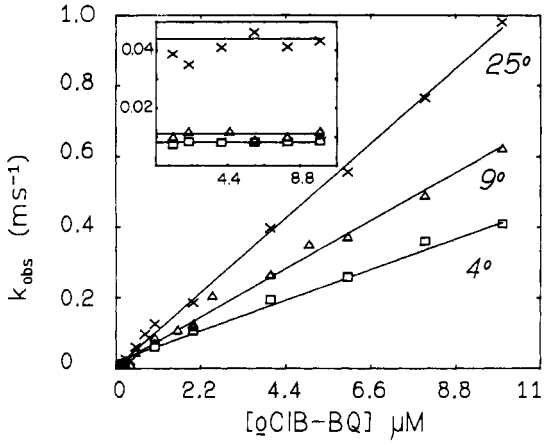

FIGURE 3: Pseudo-first-order rate constants for the association between *o*ClB-BQ and AcChE (0.2 μM) as a function of ligand concentration. Two phases in the association kinetics were evident and are plotted separately. (□) Bimolecular phase at 4 °C; (△) bimolecular phase at 9 °C; (×) bimolecular phase at 25 °C. Inset: (□) unimolecular phase at 4 °C; (△) unimolecular phase at 9 °C; (×) unimolecular phase at 25 °C.

Table II: Kinetic Constants Obtained for the Unimolecular Step in the Association Kinetics Measured at Two Ligand Concentrations[a]

compd	ligand concn (μM)	pseudo-first-order rate constant (s^{-1})
*o*ClB-BQ	1.0	39
	10.0	44
B-BQ	8.0	43
	80.0	46
DAP	12.0	33
	120.0	37
pNO_2B-BQ	12.0	27
	300.0	28
Et_3-BQ	4.0	47
	30.0	41
Me_3-BQ	50.0	46
	500.0	30
ambenonium	1.0	26
	10.0	34

[a] AcChE concentration was 0.2 μM for all of the reactions.

slope of zero, which demonstrates that its rate is independent of ligand concentration. Slopes of the fast component, intercept values for the slower component, and relative amplitudes at various temperatures are presented in Table I.

Unimolecular Steps Observed for Other Bisquaternary Ligands. Four other bisquaternary benzoquinone ligands and 1,10-bis(3-aminopyridinio)decane (Chart I) were examined to determine if the slow, concentration-independent rates were apparent with other congeners. AcChE (0.2 μM) was rapidly mixed with these ligands at two ligand concentrations which differed by 1 order of magnitude. The results presented in Table II indicate that a slow unimolecular rate is a common feature of all bisquaternary ligands examined in which the distance between the quaternary nitrogens is 14 Å. The magnitude of the unimolecular rate (27–47 s^{-1}) appears to be independent of the nature of the quaternary N-substitution for bisquaternary ligands whose equilibrium dissociation constants (Taylor & Jacobs, 1974) range over 3 orders of magnitude.

Dissociation Kinetics Measured by Competition with Decamethonium. When the ligand–AcChE complex, AcChE·L_1, is mixed with a high concentration of a second ligand, L_2, which competes at the same binding site, the following equation should describe the ensuing reaction.

Scheme I

$$L + AcChE \underset{k_{-1}}{\overset{k_1}{\rightleftharpoons}} (L\cdot AcChE)_1 \underset{k_{-2}}{\overset{k_2}{\rightleftharpoons}} (L\cdot AcChE)_2 \quad (2)$$

Scheme II

$$L + (AcChE)_1 \underset{k_{-3}}{\overset{k_3}{\rightleftharpoons}} L\cdot AcChE \quad (3)$$

$$k_4 \uparrow\downarrow k_{-4}$$

$$(AcChE)_2$$

$$AcChE\cdot L_1 \quad k_{1d} \downarrow\uparrow k_{1a}$$

$$AcChE + L_2 \underset{k_{2d}}{\overset{k_{2a}}{\rightleftharpoons}} AcChE\cdot L_2$$

$$+$$

$$L_1$$

If $k_{2a}[L_2] \gg k_{1a}[L_1]$ and $k_{2a}[L_2] \gg k_{1d}$ and if a ternary complex does not form, the conversion kinetics from AcChE·L_1 to AcChE·L_2 is rate-limited by k_{1d}. To achieve these conditions for dissociation of the benzoquinone·AcChE complexes, we have employed 4 mM decamethonium (K_D = 6 μM). The binding of benzoquinone and decamethonium is competitive, and the high concentration of decamethonium employed should allow the above kinetic constraints to prevail. The observed increase in fluorescence is a consequence of the replacement of the benzoquinone ligand by the nonquenching decamethonium. Dissociation rates were found to be independent of decamethonium concentration in the range of 80 μM–4 mM, confirming that the rate limitation is the dissociation of L_1 (Table III).[2]

Description of the Reaction Kinetics. The kinetic findings indicate that two distinct species of AcChE are revealed upon bisquaternary ligand complexation. Since quenching by the benzoquinone analogues is dominated by a dipolar energy transfer mechanism (Taylor & Jacobs, 1974), cf. Figure 1b, it is likely that formation of the initial complex gives rise to the largest signal change. Thus, the difference in the fluorescence signal between free and ligand-complexed enzyme is likely to be greater than the difference in the signal between the two putative enzyme states [$(AcChE)_1$ and $(AcChE)_2$] or between the two complexes [L·$(AcChE)_1$ and L·$(AcChE)_2$]. Two minimal schemes for describing the kinetics are shown (Scheme I and Scheme II). In Scheme I a change in conformation of the enzyme–ligand complex follows ligand complexation while in Scheme II the enzyme exists in two

[2] Similar measurements of the dissociation rates were determined using 50 μM ambenonium (K_D < 4 nM) as the dissociating ligand, and an equivalent signal change indicative of complete dissociation of the benzoquinone–AcChE complex was observed. For the high-affinity ligand *o*ClB-BQ, the dissociation rates were independent of ambenonium concentration from 0.2 to 50 μM. However, the dissociation rates of the lower affinity ligands *p*NO_2B-BQ and Et_3-BQ were substantially affected by the concentration of ambenonium used for the dissociation reaction. This result suggests that a ternary complex may be involved in the reaction of the benzoquinone·AcChE complex with high concentrations of ambenonium. Therefore, these observed dissociation rates would not reflect the intrinsic rate of dissociation for the lower affinity ligands. When decamethonium or ambenonium was used as the quenching competing ligand, a single exponential described the dissociation kinetics for all ligands except *p*-NO_2B-BQ where we observed deviations from first-order kinetics.

Table III: Dissociation Rate Constants Obtained by Dissociation of the BQ·AcChE Complex by Decamethonium[a]

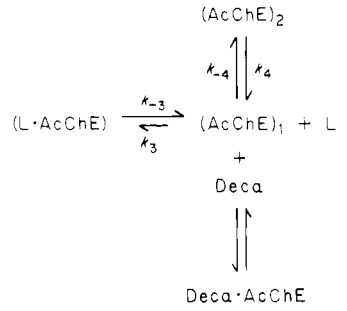

ligand	dissocn k_{obsd} (s^{-1})	measured K_d[b] (μM)	calcd K_d[c] (μM)
*o*ClB-BQ	1.2	0.028	0.020
B-BQ	11.2	0.19	0.19
DAP	19.0	0.30	0.32
pNO_2B-BQ[d]	116	2.90	1.94
Et_3-BQ	275	3.10	4.61
Me_3-BQ[d]	526	12.0	8.81

[a] The kinetic scheme shown above was assumed, where Deca is 4 mM decamethonium. The enzyme concentration is 0.5 μM and the ligand L is present in concentrations to achieve 95% binding prior to addition of decamethonium. [b] Taylor & Jacobs (1974). [c] Calculated from the equation $K_d = (1 + k_{-4}/k_4)/(k_3/k_{-3})$ and assuming $k_1 = 9.7 \times 10^7$ M^{-1} s^{-1} and $k_{-4}/k_4 = 0.62$ at 25 °C. [d] Decamethonium concentration was 3 mM for these two ligands.

states prior to ligand association and only one state binds the ligand. If $(k_1[L] + k_{-1}) \gg (k_2 + k_{-2})$ or $(k_3[L] + k_{-3}) \gg (k_4 + k_{-4})$, then both schemes are consistent with the observation of rapid quenching, followed by a slower quenching step, the rate of the latter step being independent of ligand concentration.

If the signal change arises from the ligand complexation step ($k_1 + k_{-1}$ in Scheme I and $k_3 + k_{-3}$ in Scheme II), Scheme I requires that the amplitude of the fast component increases in proportion to the amount of transient intermediate formed ($k_1[L]/k_{-1}$) and that the amplitude of the slow component would be proportional to the amount of free enzyme remaining after the initial rapid bimolecular reaction. On the other hand Scheme II requires that the amplitudes of the two components have a constant ratio when $k_3[L]$ exceeds ($k_4 + k_{-4}$). Consistent with the latter scheme, we find that at three temperatures the amplitudes of the fast and slow phases remain constant over a 10-fold ligand concentration range (Table I). Second, when the reaction was run with AcChE in stoichiometric excess over *o*-ClB-BQ, the amplitude of the fast component approached 100% of the total signal. This relationship between the fractional amplitude of the fast phase and the stoichiometry of reactants is shown in Figure 4. Finally, the lack of dependence of the isomerization rate on ligand structure is consonant with isomerization of the free enzyme. Clearly, these results, when taken together, provide strong support for a mechanism involving isomerization of the free enzyme rather than the enzyme–ligand complex. Thus, Scheme II is the likely minimal mechanism consistent with the stopped-flow data.

Calculation of Dissociation Constants and Computer Modeling of Scheme II. The equilibrium constants derived from the four experimentally determined kinetic constants in Scheme II are in close accord with the equilibrium constants previously determined from equilibrium fluorescence titrations. Dissociation rate constants for six bisquaternary compounds measured as described previously were utilized in conjunction with the measured bimolecular association constant (9.7×10^7 M^{-1} s^{-1}) and the ratio of k_{-4}/k_4 (0.62) for *o*ClB-BQ at 25 °C to calculate their corresponding equilibrium dissociation constants. There is good agreement between these calculated equilibrium constants and the values measured previously from equilibrium titrations (Taylor & Jacobs, 1974) (Table III).

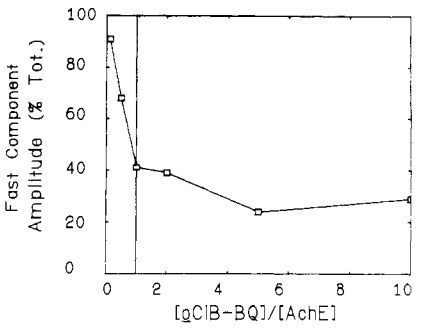

FIGURE 4: Effect of the ratio of stoichiometry of reactants (*o*ClB-BQ/AcChE) on the percentage of the total quenching signal occurring as the fast component. Measurements were conducted in the high ionic strength buffer at 8 °C.

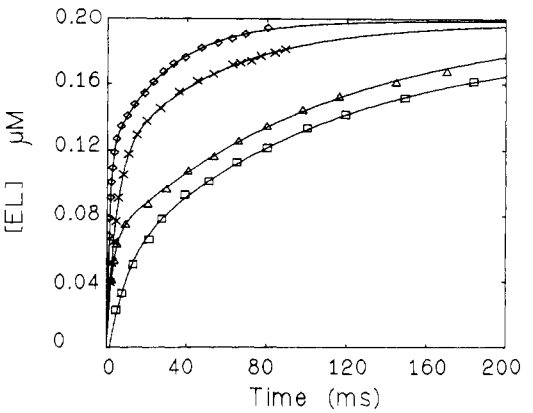

FIGURE 5: Curve fitting applied to kinetics for *o*ClB-BQ association with AcChE. The equation utilized (cf. Appendix) represents the analytical solution to three differential equations describing the kinetic equations outlined in Scheme II where EL is the ligand–enzyme complex. In each experiment the concentration of AcChE was 0.2 μM; (◇) *o*ClB-BQ (10 μM) at 25 °C; (×) *o*ClB-BQ (1 μM) at 25 °C; (△) *o*ClB-BQ (10 μM) at 4 °C; (□) *o*ClB-BQ (1 μM) at 4 °C. The average values for rate constants determined for six concentrations are, at 25 °C, $k_3 = 1.2$ (±0.6) $\times 10^8$ M^{-1} s^{-1}, $k_{-3} = 1.2$ s^{-1}, $k_4 = 33.9$ (±8.5) s^{-1}, and $k_{-4} = 20.9$ (±7.1) s^{-1} and, at 4 °C, $k_3 = 6.2$ (±2.5) $\times 10^7$ M^{-1} s^{-1}, $k_{-3} = 0.36$ s^{-1}, $k_4 = 10.0$ (±0.7) s^{-1}, and $k_{-4} = 17.8$ (±4.6) s^{-1}.

In addition, nonlinear regression analysis was used to estimate k_3, k_4, and k_{-4} by fitting to the observed *o*ClB-BQ association data (Figure 5) curves obtained from an equation which represents the analytical solution to the three differential equations describing reaction Scheme II [Rodiguin & Rodiguina (1964) and Appendix]. The average values for rate constants at 25 °C determined for six concentrations are $k_3 = 1.2$ (±0.6) $\times 10^8$ M^{-1} s^{-1}, $k_{-3} = 1.2$ s^{-1}, $k_4 = 33.9$ (±8.5) s^{-1}, and $k_{-4} = 20.9$ (±7.1) s^{-1}. The K_d for *o*ClB-BQ calculated from the latter procedure is 1.6×10^{-8} M, a value which is also in good accord with the equilibrium titrations (Table III).

Propidium Binding and Dissociation. The structurally distinct and peripheral site selective ligand propidium diiodide contrasts with the aforementioned bisquaternary ligands in its kinetic behavior. All kinetic measurements for propidium were conducted in low ionic strength buffer (1 mM Tris-HCl, pH 8.0) because at that ionic strength the affinity of propidium ($K_d = 3 \times 10^{-7}$ M) is 10 times higher than at high ionic strength where the dissociation rate is too rapid for stopped-flow measurement (Taylor & Lappi, 1975). When pseudo-first-

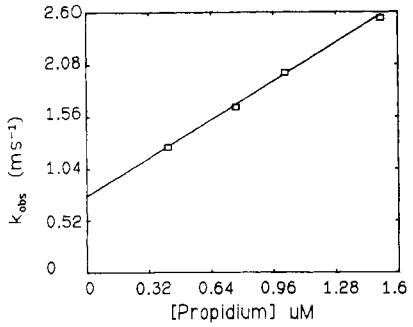

FIGURE 6: Rate of association of propidium diiodide with AcChE. The enzyme was present at concentrations between 0.1 and 0.5 μM to achieve pseudo-first-order conditions. Sample buffer was 0.001 M Tris-HCl, pH 8.0, and the temperature was 19 °C.

Table IV: Kinetic Constants Measured at Various Temperatures for Association of *o*ClB-BQ with AcChE[a]

temp (°C)	k_3 (M^{-1} s^{-1})	k_{-3} (s^{-1})	k_4 (s^{-1})	k_{-4} (s^{-1})	K_3 (M^{-1})	K_4	K_d (M)
25	9.7×10^7	1.2	27.1	16.9	8.1×10^7	1.6	2.0×10^{-8}
9	6.2×10^7	0.7	4.3	6.8	8.9×10^7	0.6	2.9×10^{-8}
4	3.9×10^7	0.4	2.9	6.1	9.9×10^7	0.5	3.2×10^{-8}
r^2 [b]	0.95	0.95	0.99	0.99	0.95	0.99	0.99

[a] Kinetic constants refer to those in Scheme II. $K_4 = k_4/k_{-4}$, $K_3 = k_3/k_{-3}$, and $K_d = (1 + 1/K_4)/K_3$. [b] Slopes, intercepts, and coefficients of determination (r^2) were determined from simple linear regression applied to the Arrhenius (ln k vs. $1/T$) and van't Hoff plots (ln K_a vs. $1/T$) of the above data.

order conditions are maintained for a variety of enzyme and ligand concentrations, the directly observed rate constants for propidium binding to AcChE can be obtained by monitoring the enhancement in propidium fluorescence at λ_{em} = 602 nm when excited at either 290 ($\epsilon_{288}^M = 5.6 \times 10^4$) or 535 nm ($\epsilon_{494}^M = 6.1 \times 10^3$) (Figure 6). Propidium does not exhibit biphasic kinetics when studied up to reaction half-times of 280 μs. By assuming a simple bimolecular association model for the binding of propidium to AcChE, we can determine the rate constants k_1 and k_{-1} from the slope and intercept of the concentration-dependence plot in Figure 5. The slope of 1.2 $\times 10^9$ M^{-1} s^{-1} is consistent with the rate of association of propidium being limited by diffusion. The intercept is 764 s^{-1} which would represent the dissociation rate by assuming the model above. The dissociation rate at 19 °C was also measured directly by competition with ambenonium at two concentrations (10 μM, k_{-1} = 546 s^{-1}; 50 μM, k_{-1} = 535 s^{-1}). The association and dissociation rate constants can be used to calculate the equilibrium dissociation constant 5.1×10^{-7} M which is in good accord with the measured dissociation constant of 3.0×10^{-7} M (Taylor & Lappi, 1975).

Temperature Dependence of Rate Constants. The temperature dependences of the respective rate constants were analyzed according to the formulas

$$\ln k = \ln \left(\frac{k'T}{h} e^{-E_a/RT} e^{\Delta S^\ddagger/R} \right) \quad (4)$$

$$\Delta H^\ddagger = E_a - RT \quad (5)$$

$$\Delta G^\ddagger = \Delta H^\ddagger - T\Delta S^\ddagger \quad (6)$$

where k' is Boltzmann's constant, h is Planck's constant, and $\Delta G^\ddagger$, $\Delta H^\ddagger$, and $\Delta S^\ddagger$ represent the activation free energy, enthalpy, and entropy, respectively. For *o*ClB-BQ, the rate constants were determined at three temperatures (Table IV). Arrhenius plots were found to be linear with correlation coefficients not less than 0.95.

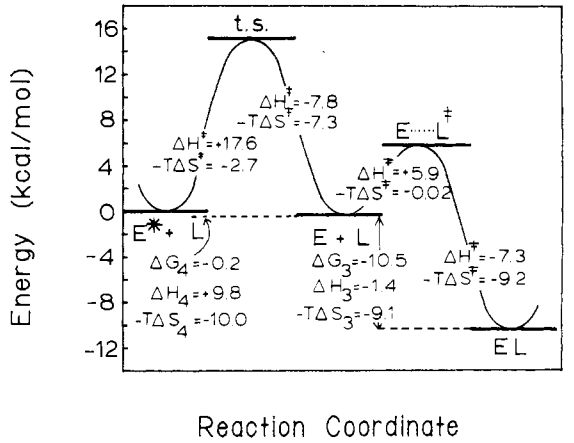

FIGURE 7: Reaction coordinate profile for *o*ClB-BQ interaction with AcChE. The profile was generated from analysis of the temperature dependence of the rate constants for each step in Scheme II (cf. Table IV).

Discussion

Mechanism of Bisquaternary Ligand Binding. Three distinct lines of evidence have emerged from the kinetic analysis, indicating that bisquaternary ligands bind to one of two preexistent enzyme conformations (Scheme II). First, when the reaction is run with ligand in stoichiometric deficiency of the enzyme, only the rapid step in the association kinetics is observed (Figure 4). Second, the rate of the isomerization step is essentially independent of bisquaternary ligand structure (Table II). Finally, the kinetic data can be fit to an equation derived from the scheme involving isomerization of the free enzyme where the equilibrium constant calculated from the kinetics is in good accord with the value obtained from equilibrium titrations (Appendix).

Active and Peripheral Site Binding Kinetics. It is instructive to compare the association and dissociation kinetics of the bisquaternary compounds studied here with respect to those found for the active site and peripheral site selective compounds, *N*-methylacridinium and propidium. Propidium binding to AcChE is characterized by an association rate (1.2×10^9 M^{-1} s^{-1}) of sufficient magnitude to be diffusion-limited or dominated by the initial encounter (Alberty & Hammes, 1958). Despite its binding to a different site, the *N*-methylacridinium association rate is of similar magnitude, k_{obsd} = 1.2×10^9 M^{-1} s^{-1} (Rosenberry & Neumann, 1977). Hence, the binding of both peripheral and active site selective ligands appears diffusion-controlled and requires minimal alteration in protein structure to pass through the transition state. Typically, diffusion- or encounter-controlled reactions possess $\Delta H^\ddagger$ values of 3–4 kcal/mol (Burgen, 1966). In contrast, the bisquaternary ligand *o*ClB-BQ, with a slower apparent bimolecular rate (k_{obsd} = 9.7×10^7 M^{-1} s^{-1}), requires substantial changes in free energy and enthalpy of activation (cf. Figure 7) to traverse activation barriers encountered in both the bimolecular and the unimolecular steps. Hence, it is likely that a change in conformation, in addition to selection of one of the two existing enzyme forms, is necessary to accommodate the binding of bisquaternary ligands.

The largest contribution to the total free energy change for complex formation (ΔG_3) arises from the change in entropy ($-T\Delta S_3$) (Figure 7). This suggests that the driving force for complex formation is related to hydrophobic interactions between the ligand and AcChE. Hydrophobic interactions have been observed to produce large positive entropy changes

due to desolvation of the ligand and its binding site during complex formation for glucocorticoid receptors and for binding of trypsin to a trypsin inhibitor (Wolff et al., 1978; Jencks, 1969; Janin & Chothia, 1976). It should also be noted that although the change in free energy produced by the enzyme isomerization (ΔG_4) calculated at 25 °C is small (−0.2 kcal/mol), the magnitude of the enthalpic and entropic contributions is opposing and large. The entropic contribution ($-T\Delta S_4 = -10.0$ kcal/mol) suggests that the driving force for isomerization of the enzyme to a form which binds bisquaternary ligands arises from hydrophobic interactions and the return of structured water to bulk solvent. The increase in enthalpy of activation (+17.6 kcal/mol) observed on the path to the transition state for the isomerization of the enzyme indicates that large amounts of energy are absorbed, leading to a conformation which can bind to bisquaternary ligands. The thermodynamic parameters obtained for AcChE isomerization are reminiscent of values found for hydrophobic bond formation which accompanies protein folding [cf. Scheraga (1978)].

Structure in Relation to Kinetics. One can speculate from a structural point of view about the nature of the observed binding forces and about why bisquaternary ligands whose interquaternary distance is 14 Å, in contrast to active and peripheral site ligands, distinguish two interconvertible forms of the enzyme. Large increases in entropy would be expected for desolvation of each of the bulky quaternary nitrogen cations analogous to the change in entropy observed when nonpolar solutes interact in an aqueous medium (Jencks, 1969). Also, critical alignment of the quaternary ammonium groups with complementary anionic sites in the protein would be required for the production of close-range electrostatic interactions. Thus, if the distance between active and peripheral sites in the native enzyme is greater than 14 Å, the rate of bimolecular association, which is slower than that observed for either *N*-methylacridinium or propidium, and the observed unimolecular step both could involve realignment of the anionic sites of the protein to come in apposition with the bisquaternary ligands. By this criterion, binding of ligands specific for the active or peripheral sites would not be expected to require these same changes in enzyme conformation. Consistent with diffusion-limited kinetics, the emission spectra of AcChE when complexed to *N*-methyacridinium or propidium do not exhibit a blue shift of the emission maxima for tryptophan fluorescence of the AcChE–ligand complex.

Acknowledgments

We thank Dr. P. B. Chock for his helpful discussions and for allowing us to run some of the fast kinetic studies on his instrumentation.

Appendix

Assuming that the predominate signal change arises from direct Förster energy transfer from tryptophanyl residues to the benzoquinone ligand, one would expect the signal differences to result from the ligand complexation step (step 3 in Scheme II) rather than from isomerization of the free enzyme or isomerization of the enzyme–ligand complex. The analytical solution to the following three differential equations which describe Scheme II was obtained by application of the La Place–Carson method of originals and transforms (Rodiguin & Rodiguina, 1964). In the following model the symbol k_3 represents k_3[L] from Scheme II.

$$\frac{d[(AcChE)_2]}{dt} = k_{-4}[(AcChE)_1] - k_4[(AcChE)_2] \quad (A1)$$

$$\frac{d[(AcChE)_1]}{dt} = k_4[(AcChE)_2] - k_{-4}[(AcChE)_1] - k_3[(AcChE)_1] + k_{-3}[L\cdot AcChE] \quad (A2)$$

$$\frac{d[L\cdot AcChE]}{dt} = k_3[(AcChE)_1] - k_{-3}[L\cdot AcChE] \quad (A3)$$

The result is an expression for the concentration of bound enzyme ([L·AcChE]) with respect to time

$$[L\cdot AcChE] = k_3[(AcChE)_1]_0\frac{b}{\gamma_1\gamma_2} - \frac{b-\gamma_1}{\gamma_1(\gamma_2-\gamma_1)e^{-\gamma_1 t}} - \frac{b-\gamma_2}{\gamma_2(\gamma_1-\gamma_2)e^{-\gamma_2 t}}$$

where γ_1 and γ_2 are the roots of the quadratic equation $\gamma^2 + \gamma(k_3 + k_{-3} + k_4 + k_{-4}) + k_{-3}(k_4 + k_{-4}) + k_3k_4$ taken with reverse signs and $b = k_4[(AcChE)_2]_0/[(AcChE)_1]_0 + k_4$. The dissociation rates ($k_{-3}^{25°C} = 1.2$ s^{-1}; $k_{-3}^{4°C} = 0.4$ s^{-1}) were measured directly and applied to the solution as constants. The following three parameters were determined by nonlinear least-squares regression analysis using a program based on the method of Marquardt (1963).

$$\text{parameter 1} = [(AcChE)_2]_0/[(AcChE)_1]_0$$

$$\text{parameter 2} = k_3$$

$$\text{parameter 3} = k_4 + k_{-4}$$

Minimization of the sum of squares was carried out until the change in parameter values was 1×10^{-3} or the change in the sum of squares < (1×10^{-4} times the final value). From the best fit values of the parameters, the isomerization rate constants were obtained from the following equations.

$$k_4 = \text{parameter 3}/(1 + \text{parameter 1})$$

$$k_{-4} = \text{parameter 3}/(1 + 1/\text{parameter 1})$$

The results of the curve-fitting program evaluated (with the Tektronics 4051 computer) for association of 2,5-bis[[3-[diethyl(*o*-chlorobenzyl)ammonio]propyl]amino]benzoquinone (*o*ClB-BQ) at four concentrations are shown in Figure 5. The average values for rate constants at 25 °C determined for six concentrations are $k_3 = 1.2\ (\pm 0.6) \times 10^8$ M^{-1} s^{-1}, $k_{-3} = 1.2$ s^{-1}, $k_4 = 33.9\ (\pm 8.5)$ s^{-1}, and $k_{-4} = 20.9\ (\pm 7.1)$ s^{-1}.

The K_d for the association of *o*ClB-BQ can be calculated from the following equation.

$$K_d = \frac{1 + k_{-4}/k_4}{k_3/k_{-3}} = 1.6 \times 10^{-8}\ \text{M}$$

This value is in good agreement with the measured K_d from equilibrium fluorescence titrations (2.8×10^{-8} M). Thus, a two-state model involving an enzyme isomerization appears appropriate for bisquaternary ligand binding to AcChE.

References

Alberty, R. A., & Hammes, G. G. (1958) *J. Phys. Chem. 62*, 154–159.
Berman, H. A., & Taylor, P. (1978) *Biochemistry 17*, 1704–1712.
Burgen, A. S. V. (1966) *J. Pharm. Pharmacol. 18*, 137–149.
Changeux, J.-P. (1966) *Mol. Pharmacol. 2*, 369–392.
Förster, T. (1965) in *Modern Quantum Chemistry* (Sinanoglu, O., Ed.) Part 3, pp 93–137, Academic Press, New York.
Janin, S., & Chothia, C. (1976) *J. Mol. Biol. 100*, 197–211.
Jencks, W. P. (1969) in *Catalysis in Chemistry and Enzymology*, pp 422–427, McGraw-Hill, New York.
Kato, G. (1972) *Mol. Pharmacol. 8*, 582–588.

Marquardt, D. W. (1963) *J. Soc. Ind. Appl. Math. 2*, 431–441.
Mooser, G., & Sigman, D. S. (1974) *Biochemistry 13*, 2299–2307.
Mooser, G., Schulman, H., & Sigman, D. S. (1972) *Biochemistry 11*, 1595–1602.
Rhee, S. G., & Chock, P. B. (1976) *Biochemistry 15*, 1755–1760.
Rodiguin, N. M., & Rodiguina, E. N. (1964) in *Consecutive Chemical Reactions* (Schneider, R. T., Ed.) pp 24–26, Van Nostrand, Princeton, NJ.
Rosenberry, T. L., & Neumann, E. (1977) *Biochemistry 16*, 3870–3878.
Scheraga, H. A. (1978) *Acc. Chem. Res. 12*, 7–14.
Stryer, L. (1968) *Science 162*, 526–533.
Taylor, P., & Jacobs, N. M. (1974) *Mol. Pharmacol. 10*, 93–107.
Taylor, P. W., & Lappi, S. (1975) *Biochemistry 14*, 1989–1997.
Taylor, P., Jones, J. W., & Jacobs, N. M. (1974) *Mol. Pharmacol. 10*, 78–92.
Wee, V. T., Sinha, B. K., Taylor, P. W., & Chignell, C. F. (1976) *Mol. Pharmacol. 12*, 667–677.
Wolff, M. E., Baxter, J. D., Kollman, P. A., Lee, D. L., Kuntz, I. D., Bloom, E., Matulich, D. T., & Morris, J. (1978) *Biochemistry 16*, 3201–3208.

Time-Resolved Resonance Raman Characterization of the bO_{640} Intermediate of Bacteriorhodopsin. Reprotonation of the Schiff Base†

James Terner,‡ Chung-Lu Hsieh, Alan R. Burns, and M. A. El-Sayed*

ABSTRACT: The resonance Raman spectrum of photolyzed bacteriorhodopsin under conditions known to increase the concentration of the bO_{640} intermediate in both H_2O and D_2O is presented. By use of computer subtraction techniques and a knowledge of the Raman spectra of the unphotolyzed bacteriorhodopsin as well as the other intermediates in the cycle, a qualitative spectrum of bO_{640} is determined. The shift of a band at 1630 cm^{-1} in H_2O to 1616 cm^{-1} in D_2O suggests that the Schiff base of bO_{640} is protonated. Additional bands at 947, 965, and 992 cm^{-1} that appear only in D_2O suspensions confirm that a proton is coupled to the retinal chromophore of bO_{640}. The reprotonation of the Schiff base thus occurs during the bM_{412} to bO_{640} step. The fingerprint region, sensitive to the isomeric configuration of the retinal chromophore of bO_{640}, is dissimilar to the fingerprint regions of published model compounds and other forms of bacteriorhodopsin.

Upon illumination, bacteriorhodopsin, a retinal protein complex similar in structure to the visual pigments (Oesterhelt & Stoeckenius, 1971), has been shown to undergo a cyclic transformation through several intermediates (Lozier et al., 1975). The net effect of the cycle is the transport of protons from the inside of the bacterial cell membrane to the outside, which sets up an electrochemical gradient that is thought to drive the synthesis of ATP (Oesterhelt, 1976). The intermediates of bacteriorhodopsin (Figure 1) were first characterized by time-resolved optical absorptions [for a recent review see Stoeckenius et al. (1979)] and are now being characterized by resonance Raman spectroscopy. The vibrational spectra are capable of providing more detailed structural information than are the broad absorption bands. In particular, the protonation state of the Schiff base linkage between the retinal and the lysine residue and the isomeric configuration of the retinal have received the most attention. At the present time, complete resonance Raman spectra have been obtained of the bR_{560}^{DA} (Terner & El-Sayed, 1978; Marcus & Lewis, 1978; Terner et al., 1979a), bR_{570} (Terner et al., 1977; Aton et al., 1977; Marcus & Lewis, 1978), bL_{550} (Terner et al., 1979a), bM_{412} (Terner et al., 1977; Aton et al., 1977; Marcus & Lewis, 1978), and bK_{590} (Terner et al., 1979b) components of the cycle. In this paper we present the complete resonance Raman spectrum of the retinal chromophore of the bO_{640} intermediate and discuss the evidence for its protonation state as well as conformation changes during the cycle.

Experimental Procedures

Materials

Samples. Purple membrane isolated from *Halobacterium halobium* R_1 was the gift of Dr. R. A. Bogomolni and Professor W. Stoeckenius of the University of California, San Francisco, San Francisco, CA. Refrigerated samples were illuminated by a tungsten lamp for several weeks until sufficient carotenoid was photooxidized so that the carotenoid Raman bands at 1255 and 1515 cm^{-1} were no longer detectable (Terner et al., 1979a). Samples were placed in short lengths of melting point capillary tubes at approximately 50 μM in distilled water or D_2O (Bio-Rad). The capillaries were mounted inside a flowing-water jacket and maintained at 40 °C. Considerable enhancement of some of the Raman bands was observed at this temperature, relative to room temperature. Since the optical absorption of the bO_{640} intermediate was similarly enhanced (Lozier et al., 1975), we have assigned the corresponding Raman bands to the bO_{640} intermediate.

Apparatus. The excitation system used for this experiment consisted of a Spectra-Physics Model 375 dye laser pumped

† From the Department of Chemistry, University of California, Los Angeles, Los Angeles, California 90024. *Received January 29, 1979.* This work was supported by the Department of Energy, Office of Basic Energy Sciences.
‡ Partially supported by a National Science Foundation National Needs Traineeship.

0006-2960/79/0418-3629$01.00/0